Hydrogenation of the ternary silicides RENiSi (RE = Ce, Nd) crystallizing in the tetragonal LaPtSi-type structure

Mathieu Pasturel, François Weill, Françoise Bourée, Jean-Louis Bobet, Bernard Chevalier

▶ **To cite this version:**

Mathieu Pasturel, François Weill, Françoise Bourée, Jean-Louis Bobet, Bernard Chevalier. Hydrogenation of the ternary silicides RENiSi (RE = Ce, Nd) crystallizing in the tetragonal LaPtSi-type structure. Journal of Alloys and Compounds, 2005, 397 (1-2), pp.17-22. 10.1016/j.jallcom.2005.01.015 . hal-00090761

HAL Id: hal-00090761
https://hal.science/hal-00090761

Submitted on 13 Feb 2024

HAL is a multi-disciplinary open access archive for the deposit and dissemination of scientific research documents, whether they are published or not. The documents may come from teaching and research institutions in France or abroad, or from public or private research centers.

L'archive ouverte pluridisciplinaire **HAL**, est destinée au dépôt et à la diffusion de documents scientifiques de niveau recherche, publiés ou non, émanant des établissements d'enseignement et de recherche français ou étrangers, des laboratoires publics ou privés.

Hydrogenation of the ternary silicides RENiSi (RE = Ce, Nd) crystallizing in the tetragonal LaPtSi-type structure

M. Pasturel [a], F. Weill [a], F. Bourée [b], J.-L. Bobet [a], B. Chevalier [a, *]

[a] *ICMCB, CNRS [UPR 9048], Université Bordeaux 1, 87 av.du Dr.A.Schweitzer, 33608 Pezssac Cedex, France*
[b] *LLB, CEA-CNRS, CEA Saclay, 91191 Gif-sur-Yvette, France*

Abstract

Hydrogenation of isostructural RENiSi (RE = Ce, Nd) intermetallic compounds has been performed. Neutron diffraction experiments on $CeNiSiD_{1.2(1)}$ indicates that D-atoms fully occupy the $[Ce_3Ni_2]$- and partially fill the $[Ce_3Si_2]$-bipyramidal sites. The strong hybridisation between Ce and D in these sites can explain the observed increase of the cerium valence after deuterium insertion. The magnetic phase diagram of NdNiSi has been established and highlights two antiferromagnetic transitions at $T_{N1} = 6.8(2)$ K and $T_{N2} = 2.8(2)$ K, which disappear after hydrogenation.

Keywords: Hydrogenation; Rare-earth-based intermetallics; Neutron diffraction; Magnetic phase diagram

1. Introduction

The physical properties of CeTX (T = transition element, X = p element) ternary intermetallic compounds are strongly dependent on the hybridisation strength J_{cf} between 4f(Ce) and conduction electrons. As highlighted by Doniach [1], J_{cf} governs the competition between RKKY indirect magnetic interactions [2] and the demagnetising Kondo effect [3]. Hydrogenation, which induces changes both on the interatomic distances and on the density of states at the Fermi level, has been proved to be an efficient way to modify J_{cf} and the physical behaviour of CeTX compounds. For example, in $CeIrAlH_2$, cerium is in a trivalent state while the pristine CeIrAl is a valence fluctuating compound [4].

Considering the family CeNiX (X = Al, Ga, In, Sn), hydrogenation leads to transition from intermediate valence state to trivalent state of cerium [5] with possible magnetic ordering in the case of $CeNiInH_{1.8(1)}$ [6] and $CeNiSnH_y$ ($y = 1.0(1)$ or $1.8(1)$) [7–9]. In the case of $CeNiGeH_{1.6(1)}$, the intermediate valence state remains but the Kondo effect is strongly decreased [10]. In these examples, hydrogenation acts like a negative pressure and similar modifications of physical behaviour are obtained by substituting nickel by a larger element as Pt or Pd. For example, $CeNiSnH_{1.0(1)}$ [7,9] and $CeNi_{0.4}Pt_{0.6}Sn$ [11] are antiferromagnets (both $T_N = 4.5(2)$ K), while the initial CeNiSn is a well-known Kondo semiconductor [12].

Recently, an anomalous increase of the Kondo effect was observed after hydrogenation of the ternary silicide CeNiSi [13] crystallizing in the tetragonal LaPtSi-type structure. A different site occupancy by H-atoms than the usually admitted $[Ce_3Ni]$ tetrahedrons was hypothesized to justify both the lack of significant molar volume increase ($\Delta V_m/V_m = +0.1\%$) and this unusual magnetic behaviour.

The first aim of this paper is to verify this hypothesis. We report the structural analysis of the deuteride $CeNiSiD_{1.2(1)}$ by neutron diffraction. The second aim is to report for the first time the magnetic properties of NdNiSi and $NdNiSiH_{1.0(1)}$ which crystallize in the same structural type.

* Corresponding author. Tel.: +33 5 4000 6336; fax: +33 5 4000 2761.
E-mail address: chevalie@icmcb.u-bordeaux1.fr (B. Chevalier).

2. Experimental

The synthesis of intermetallic compounds and their hydrides (or deuterides) has been described in details in previous papers, as well as analysis methods (X-ray diffraction, electrical resistivity and magnetic susceptibility measurements) [5,9,13,14].

Nevertheless, the temperature used for the deuteration of CeNiSi ($T = 523$ K) is higher than that reported to obtain $CeNiSiH_{0.8(1)}$ ($T = 323$ K) [13]. The quantity of deuterium absorbed, determined by a gravimetric method, indicates the formation of $CeNiSiD_{1.2(1)}$.

Neutron powder diffraction experiments were performed at the Orphée reactor (CEA/Saclay, France), on the two-axis diffractometer 3T2 (high-resolution powder diffraction; $\lambda = 0.1225$ nm) at 300 K. The data were analysed with the Rietveld profile method using the Fullprof program [15].

3. Results and discussion

3.1. Structural determinations on $CeNiSiD_{1.2(1)}$

The neutron diffraction patterns obtained on CeNiSi and $CeNiSiD_{1.2(1)}$ are reported in Fig. 1 and the results of the structural refinements in Table 1.

CeNiSi has been reported to crystallize in the tetragonal LaPtSi-type structure (space-group $I4_1md$, no. 109) with all atoms located in 4a sites (0 0 z). This structural type leads to a quite good refinement of its neutron diffraction pattern (Table 1).

The deuterium localization in $CeNiSiD_{1.2(1)}$ has been performed by both methods of Fourier difference and

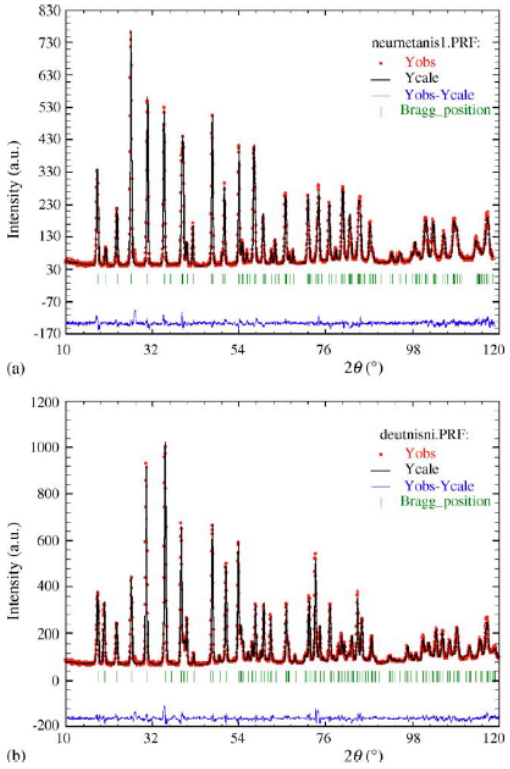

Fig. 1. Refined powder neutron diffraction patterns of (a) CeNiSi and (b) $CeNiSiD_{1.2(1)}$.

Table 1
Results of Rietveld refinement of CeNiSi and $CeNiSiD_{1.2(1)}$

		CeNiSi	$CeNiSiD_{1.2(1)}$
Space group		$I4_1md$ (no. 109)	
Cell parameters		$a = 4.0709(1)$ Å, $c = 14.0158(3)$ Å	$a = 4.0411(1)$ Å, $c = 14.2353(2)$ Å
Atomic positions (occupancy if different of 1)	Ce	0, 0, 0.000	0, 0, 0.000
	Ni	0, 0, 0.5862(3)	0, 0, 0.5821(6)
	Si	0, 0, 0.4178(4)	0, 0, 0.4171(4)
	D1 (8b)		0, 0.0790(8), 0.8343(6) (0.48(1))
	D2 (4a)		0, 0, 0.1663(7) (0.27(1))
Thermal displacement parameter	Ce	0.68(3) Å^2	0.79(5) Å^2
	Ni	0.85(2) Å^2	B11 = 0.028(2) Å^2, B12 = 0 Å^2, B22 = 0.009(2) Å^2, B13 = 0 Å^2, B33 = 0.0005(4) Å^2, B23 = 0 Å^2
	Si	0.63(4) Å^2	0.65(6) Å^2
	D1		1.33(7) Å^2
	D2		1.33(7) Å^2
Number of observed reflections		129	125
Number of refined parameters		13	31
Conventional reliability factors	R_p	0.101	0.109
	R_{wp}	0.100	0.108
	R_e	0.0561	0.0498
	χ^2	3.45	5.28
	R_{Bragg}	0.0363	0.0409
	R_f	0.0246	0.0305

Table 2
List of equivalent positions for D1 located in 8b site for $CeNiSiD_{1.2(1)}$

D1	(0, 0.0790, 0.8343)	(1/2, 0.4210, 0.3343)	(0.9210, 1/2, 0.0843)	(0.5790, 0, 0.5843)
	(0, 0.9210, 0.8343)	(1/2, 0.5790, 0.3343)	(0.0790, 1/2, 0.0843)	(0.4210, 0, 0.5843)

The two positions of a same column cannot be occupied simultaneously.

simulated annealing available with the Fullprof software. Both methods indicate the presence of deuterium atoms (D1) located in the $[Ce_3Ni_2]$ bipyramidal sites available in this structure. The refinement based on this hypothesis smoothly converges but some intensities remain unexplained.

Since the multiplicity of this site is equal to 4, the full occupation of the centre of the $[Ce_3Ni_2]$ bipyramid cannot alone explain the experimental deuterium stoichiometry. From an examination of the structure, an additional site for deuterium atoms, inside the $[Ce_3Si_2]$ bipyramids, has been hypothesized. A large improvement of the refinement results from the introduction of this D2 atom. In the structure of $CeNiInD_{0.48}$ (hexagonal ZrNiAl-type structure), Yartys et al. [16] reported a small displacement of the deuterium atoms from the centre of the $[Ce_3Ni_2]$ bipyramids. The D1 atoms had then been allowed to shift from the 4a site to a 8b $(0\,y\,z)$ site. The experimental shift ($y = 0.0790(8)$) is of the same order of magnitude than that reported by Yartys et al. Therefore, D1 atoms are located in a $[Ce_3Ni]$ tetrahedral site, very close to the $[Ce_3]$ basis. Obviously, from an interatomic distances point of view, only half of the equivalent positions can be filled, as summarized in Table 2.

The final refinement (Table 1) has been made considering anisotropic displacement parameters for Ni-atoms. A Hamilton test [17] between this hypothesis and the previous one with isotropic displacement parameters for all atoms validates the significance of the improvement of the refinement.

A projection of the structure along the [1 0 0]-direction is shown in Fig. 2 and highlights the sites occupied by deuterium atoms in this structure type as determined by neutron diffraction experiments.

Concerning the cell parameters, the a parameters of CeNiSi and $CeNiSiD_{1.2(1)}$ are in perfect agreement with those reported previously [13], while the c parameter is −0.1% smaller, both for CeNiSi and the deuteride. The difference between the concentrations in hydrogen or deuterium do not seem to influence the cell parameters.

The interatomic distances between cerium and deuterium atoms (2.35–2.38 Å) (Table 3) are close to those reported previously in hydrides based on cerium. For example, $d_{Ce-D} = 2.371(2)$ Å in $CeNiInD_{1.24}$ [16] and $d_{Ce-H} = 2.410$ Å in CeH_2 [18].

The shift from the initial 4a position to an 8b position leads to two nickel–deuterium distances. The smallest one (1.70 Å) is of an order of magnitude as those reported in intermetallic hydrides. For example, $d_{Ni-D} = 1.622$ Å in $TbNiSiD_{1.78}$ [19], $d_{Ni-D} = 1.694(6)$ in $CeNiInD_{0.48}$ [16] and $d_{Ni-D} = 1.619(2)$ Å in $LaNiSnD_2$ [20]. The shift of the D1 atom from 4a to 8b position may explain the anisotropic displacement parameter of nickel which tends to stabilize the structure in slightly shortening the Ni–D1 interatomic distance.

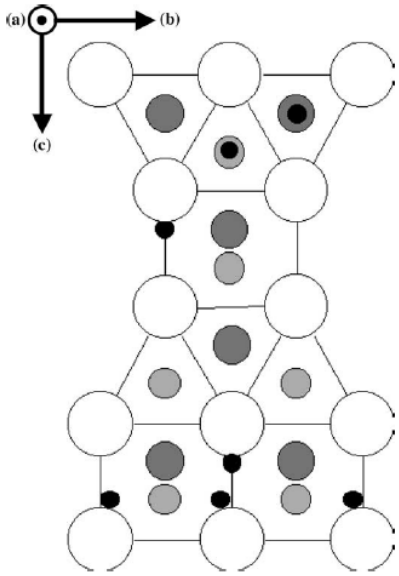

Fig. 2. Projection of the $CeNiSiD_{1.2(1)}$ structure along the [1 0 0]-direction, as determined by neutron diffraction (Ce: white large circles, Ni: light grey medium circles, Si: dark grey medium circles, D: black small circles).

Considering the refined occupancy rates of D1 (0.48(1)) and D2 (0.27(1)) sites, one can conclude that the $[Ce_3Ni_2]$

Table 3
Interatomic distances in CeNiSi and its deuteride calculated from results of Table 1

		CeNiSi	$CeNiSiD_{1.2(1)}$
Interatomic distances (Å)	Ce–4Ce	4.05	4.04
	Ce–4Ce	4.07	4.09
	Ce–4Si	3.10	3.09
	Ce–2Si	3.11	3.12
	Ce–4Ni	3.12	3.09
	Ce–2Ni	3.07	3.13
	Ce–2D1		2.37
	Ce–1D1		2.38
	Ce–2D2		2.35
	Ce–1D2		2.37
	Si–2D2		2.02
	Ni–2D1		1.79 or 2.34

triangle-based bipyramids are close to be entirely filled by D1-atom while less than one-third of [Ce_3Si_2] bipyramids are occupied. The concentration in deuterium deduced from these rates is $CeNiSiD_{1.23(3)}$, in perfect agreement with the experimental value.

The magnetic susceptibility of $CeNiSiD_{1.2(1)}$ measured at 300 K ($\chi_m = 6.5 \times 10^{-4}$ emu/mol) is comparable to the value reported for the hydride ($\chi_m = 5.9 \times 10^{-4}$ emu/mol) highlighting no strong influence of hydrogen concentration. Both these susceptibilities are lower than that of CeNiSi ($\chi_m = 1.28 \times 10^{-3}$ emu/mol). This study confirms the increase of the Kondo effect in CeNiSi after hydrogenation which seems to be linked with the unusual site occupancy by H-atoms. They are located close to three cerium atoms and must be strongly hybridised with them, resulting in an increase of the Kondo effect. This result can be compared with hydrogenation of CeCoGe [21] where H-atoms are located in [Ce_4] pseudo-tetrahedral sites and induce a demagnetisation of the compound. When H-atoms are strongly hybridised with Ce-atoms, the chemical effect could prevail over the "negative pressure" effect.

3.2. Magnetic behaviour of NdNiSi and $NdNiSiH_{1.0(1)}$

The magnetization of NdNiSi as a function of temperature in different applied magnetic fields is reported in Fig. 3. For $\mu_0 H \leq 2.4$ T, two magnetic transitions are clearly evidenced at $T_1 = 6.8(2)$ K and $T_2 = 2.8(2)$ K (for $\mu_0 H = 0.1$ T). The transition occurring at T_1 corresponds to a maximum in the curve $M = f(T)$ which could be attributed to an antiferromagnetic ordering of the Nd^{3+} moments. This correlates with the decrease of T_1 when $\mu_0 H$ increases (from $T_1 = 6.8(3)$ K for $\mu_0 H = 0.1$ T to $T_1 = 6.0(2)$ K for $\mu_0 H = 2.4$ T). The second transition is characterized by a sharp decrease of the magnetization with temperature. T_2 is determined by the inflection point of the curve. This last result suggests a spin reorientation occurring in the antiferromagnetic state of this ternary silicide. Such a result has already been observed, for example, in $NdNi_4Sn_2$ which exhibits two transitions at $T_N = 13.0(5)$ K and $T_1 = 10.0(5)$ K [22].

For higher magnetic fields ($\mu_0 H \geq 2.8$ T), only the high-temperature transition is still observed and T_1 decreases while $\mu_0 H$ increases. Moreover, the magnetic field is opposite to the antiferromagnetic ordering and the maximum observed in the curve slowly vanishes when $\mu_0 H$ increases and the magnetic transition only induces a change in the slope of $M = f(T)$ for $\mu_0 H = 4.0$ T.

These results agree with the behaviour of the magnetization as a function of applied magnetic field at different temperatures (Fig. 4). At $T = 8$ K, $M = f(\mu_0 H)$ is represented by a straight line, corresponding to the paramagnetic state of NdNiSi. At $T = 6$ K, a small deviation to this linearity is observed for $\mu_0 H \geq 1.8(2)$ T and can be explained by an upturn of some moments that align with the magnetic field. Far below T_1 ($T = 4$ K), the magnetization of NdNiSi first increases linearly with the magnetic field, with a smaller slope than

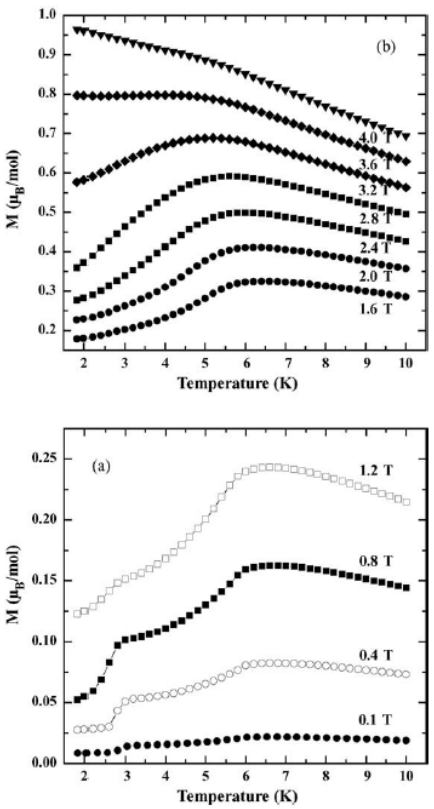

Fig. 3. Thermal dependence of the magnetization of NdNiSi in different magnetic fields applied: (a) $0.1\,T \leq \mu_0 H \leq 1.2\,T$ and (b) $1.6\,T \leq \mu_0 H \leq 4.0\,T$.

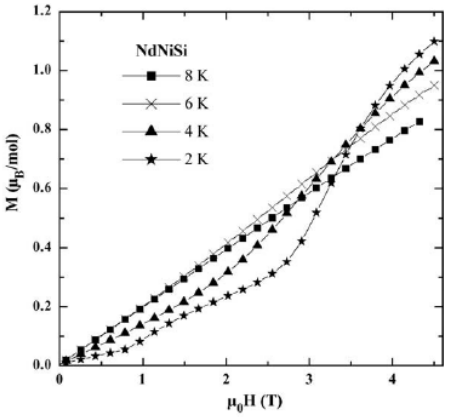

Fig. 4. Field dependence of magnetization of NdNiSi at different temperatures. The measurements have been performed by decreasing $\mu_0 H$.

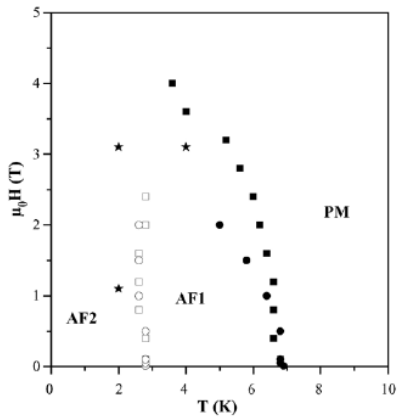

Fig. 5. Magnetic phase diagram of NdNiSi. The marks have been deduced from the curves: (■) high-temperature transition of $M=f(T)$; (□) low-temperature transition of $M=f(T)$; (⋆) $M=f(\mu_0 H)$; (●) high-temperature transition of $\chi'=f(T)$; (○) low-temperature transition of $\chi'=f(T)$.

the previous one, according to the antiferromagnetic ordering. Then, at $\mu_0 H = 3.1(2)$ T (determined by the inflection point of the curve), a strong increase of the magnetization occurs, corresponding to a metamagnetic transition probably due to a spin-flip of the Nd^{3+} moments. Finally, below T_2 ($T = 2$ K), for low magnetic fields, the slope of the linear evolution of $M=f(\mu_0 H)$ is the smallest one observed, according to the antiparallel alignment of Nd^{3+} moments. A small increase in this curve at $\mu_0 H = 1.1(2)$ T could correspond to the transition between the two antiferromagnetic states. Then, around $\mu_0 H = 3.1(1)$ K, the spin-flip occurs, inducing a sharp increase of the magnetization with the applied field.

Using all these results and measurements of a.c. susceptibility (not presented in this paper), the magnetic phase diagram of NdNiSi has been established and is presented in Fig. 5. The PM phase corresponds to the paramagnetic state, the AF1 and AF2 phases to the antiferromagnetic states. It is to be noted that the small differences observed between the T_1 temperature transition (PM → AF1) determined by d.c. and a.c. methods are mainly attributed to the precision ($\Delta T = 0.2$ K) of each measurement. The error bars have not been plotted on the graph for clarity.

The magnetization of $NdNiSiH_{1.0(1)}$ has been measured and the results are reported in Fig. 6 (Inset highlights the behaviour of the reciprocal susceptibility in the high-temperature region.) $NdNiSiH_{1.0(1)}$ perfectly follows a Curie–Weiss behaviour $1/\chi = (T+\theta_p)/C_m$ with $\theta_p = -7.5$ K and $C_m = 1.75$ emu K mol^{-1} giving an effective moment $\mu_{eff} = 3.75\mu_B$ close to the value expected for a free Nd^{3+} ion ($\mu_{eff} = 3.62\mu_B$). In the low-temperature region, no magnetic ordering is observed down to $T = 2$ K on the curve $M=f(T)$. Hydrogenation of NdNiSi induces an increase of interatomic distances, in particular d_{Nd-Nd}, which leads to a disappearance of the magnetic ordering. This result can be compared

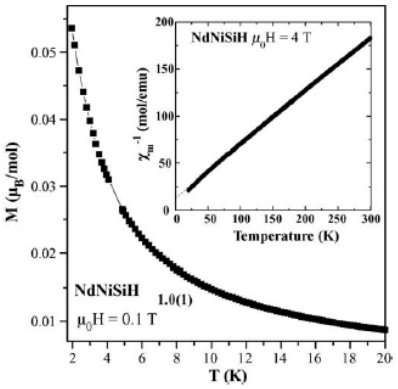

Fig. 6. Low-temperature dependence of magnetization of $NdNiSiH_{1.0(1)}$ in an applied field $\mu_0 H = 0.1$ T. The inset shows the thermal dependence of the reciprocal susceptibility in the paramagnetic region.

with those obtained on $Nd_2Fe_{14}B$ [23] where hydrogenation decreases the contribution of neodymium to the magnetisation of the compound.

4. Conclusion

Neutron diffraction performed on $CeNiSiD_{1.2(1)}$ confirms that D-atoms are inserted in [Ce_3Ni_2] but also partially in [Ce_3Si_2] bipyramids available in this structure deriving from the LaPtSi-type. The hybridisation of D-orbitals with those of cerium seems to be more pronounced than the usual case of [Ce_3Ni] tetrahedrons occupancy. This chemical effect seems to prevail over the "negative pressure" effect and must be responsible for the increase of the Kondo effect after hydrogenation.

In the case of NdNiSi, the magnetic phase diagram, dominated by antiferromagnetic interactions has been established. Hydrogenation increases the interatomic distances and $NdNiSiH_{1.0(1)}$ does not show any magnetic ordering down to 2 K. Low-temperature neutron diffraction experiments have to be performed to solve the magnetic structure of the two magnetically ordered phases of NdNiSi.

References

[1] S. Doniach, Physica B 91 (1977) 231.
[2] M.A. Rudermann, C. Kittel, Phys. Rev. 96 (1) (1954) 99.
[3] J. Kondo, Prog. Theor. Phys. 32 (1) (1964) 37.
[4] S.K. Malik, P. Raj, A. Sathyamoorthy, K. Shashikala, N.H. Kumar, L. Menon, Phys. Rev. B 63 (2001) 172418.
[5] B. Chevalier, M. Pasturel, J.-L. Bobet, R. Decourt, J. Etourneau, O. Isnard, J.S. Marcos, J.R. Fernandez, J. Alloys Compd. 383 (2004) 4.
[6] B. Chevalier, M.L. Kahn, J.-L. Bobet, M. Pasturel, J. Etourneau, J. Phys.: Condens. Matter 14 (2002) L365.

[7] V.A. Yartys, B. Ouladdiaf, O. Isnard, O.Y. Khyzhun, K.H.J. Buschow, J. Alloys Compd. 359 (2003) 62.
[8] B. Chevalier, J.-L. Bobet, M. Pasturel, E. Bauer, F. Weill, R. Decourt, J. Etourneau, Chem. Mater. 15 (2003) 2181.
[9] B. Chevalier, M. Pasturel, J.-L. Bobet, J. Etourneau, O. Isnard, J.S. Marcos, J.R. Fernandez, J. Magn. Magn. Mater. 272–276 (2004) 576.
[10] B. Chevalier, M. Pasturel, J.-L. Bobet, F. Weill, R. Decourt, J. Etourneau, J. Solid State Chem. 177 (2004) 752.
[11] J. Sakurai, R. Kawamura, T. Taniguchi, S. Nishigori, S. Ikeda, H. Goshima, T. Suzuki, T. Fujita, J. Magn. Magn. Mater. 104–107 (1992) 1415.
[12] T. Takabatake, Y. Nakazawa, M. Ishikawa, Jpn. J. Appl. Phys. 26 (Suppl. 3) (1987) 547.
[13] M. Pasturel, J.-L. Bobet, O. Isnard, B. Chevalier, J. Alloys Compd. 384 (2004) 39.
[14] J.-L. Bobet, S. Pechev, B. Chevalier, B. Darriet, J. Alloys Comp. 267 (1998) 136.
[15] J. Rodriguez-Carvajal, Powder diffraction, in: Satellite Meeting of the 15th Congress of IUCr, Toulouse, 1997, p. 127.
[16] V.A. Yartys, R.V. Denys, B.C. Hauback, H. Fjellvag, I.I. Bulyk, A.B. Riabov, Y.M. Kalychak, J. Alloys Compd. 330–332 (2002) 132.
[17] W.C. Hamilton, Acta Crystallogr. 18 (1965) 502.
[18] P. Knappe, H. Müller, Z. Anorg. Allg. Chem. 487 (1982) 63.
[19] H.W. Brinks, V.A. Yartys, B.C. Hauback, J. Alloys Compd. 322 (2001) 160.
[20] V.A. Yartys, T. Olavessen, B.C. Hauback, H. Fjellvag, H.W. Brinks, J. Alloys Compd. 330–332 (2002) 141.
[21] B. Chevalier, E. Gaudin, F. Weill, J.-L. Bobet, Intermetallics 12 (2004) 437.
[22] F. Fourgeot, B. Chevalier, P. Gravereau, J. Etourneau, Physica B 230–232 (1997) 256.
[23] J. Chaboy, C. Piquer, N. Plugaru, M. Artigas, H. Maruyama, N. Kawamura, M. Suzuki, J. Appl. Phys. 93 (1) (2003) 475.